Brazilian Journal of Geophysics (2021) 39(2): 209-226

ISSN 0102-261X
DOI: 10.22564/rbgf.v38i4.2083

HIGH-RESOLUTION MARINE SEISMIC DATA PROCESSING USING A SINGLE-CHANNEL SPARKER SYSTEM: BAHIA SHELF, BRAZIL

Italo Santos [1]*, Moab Gomes [2], German Garabito [3], Helenice Vital [2] and Victor Lopes [4]

ABSTRACT. It is still a challenge to apply fundamental seismic processing techniques, such as deconvolution and migration, to single-channel seismic data. This study proposes a processing workflow for high-resolution seismic data regarding problems of low signal/noise ratio, static variations, and multiples, which restrict the geological information of shallow strata. The data was acquired using an Applied Acoustics Squid2000 sparker system, operating up to 2500J, with a frequency range of 100-1200Hz. The survey was carried out on the continental shelf of Bahia state near the Jequitinhonha delta aiming to investigate stratigraphic structures of Quaternary deposits. The processing flow explores fundamentally the predictive deconvolution and Kirchhoff migration and applies static correction, band-pass filter, amplitude correction, and average filter. Deconvolution slightly attenuated the multiple and broadened the data frequency spectrum. Kirchhoff migration collapsed the diffraction hyperbolas, enhanced coherency and continuity of reflectors along with the data, and moved dip reflectors to a more realistic position. Static correction combined with post-stack migration and average filter smoothed the undulating seabed reflector and subsurface reflectors. The results confirmed the efficiency of the proposed workflow by the removal of random noises, correction of static variations, placement of reflectors close to their real position, and provision of a high signal/noise ratio image from the subsurface.

Keywords: subbottom profiling; shallow shelf; Kirchhoff migration; deconvolution; static correction.

RESUMO. Aplicar técnicas fundamentais de processamento sísmico, como deconvolução e migração, em dados de sísmica rasa ainda é um desafio. Este artigo propõe um fluxo de processamento para dados de sísmica rasa quanto a: baixa razão sinal/ruído; ruídos aleatórios; correção de amplitude; variações estáticas e múltiplas. Os dados foram adquiridos utilizando um sistema *sparker* da *Applied Acoustics Squid200*, potência de 2500J, faixa de frequência de 100-1200Hz. O levantamento foi realizado na plataforma continental da Bahia próximo ao delta do Rio Jequitinhonha para investigar estruturas estratigráficas rasas. O processamento explora fundamentalmente a deconvolução preditiva e a migração *Kirchhoff* e, secundariamente, a correção estática e de amplitude, filtro passa-banda e filtro de média de traço. A deconvolução atenuou levemente a múltipla, removeu ruídos aleatórios e ampliou o espectro de frequência do dado. A migração *Kirchhoff* colapsou as hipérboles de difração, aumentou a continuidade lateral dos refletores e os moveu para posições mais realistas. A correção estática sequenciada pela migração e filtro de média suavizaram o efeito ondulado dos refletores. Os resultados confirmam a eficiência do fluxo pela remoção de ruídos, correção das variações estáticas, reposicionamento de refletores e fornecimento de uma imagem sísmica de alta razão sinal/ruído de subsuperfície da plataforma continental da Bahia.

Palavras-chave: perfilagem de subfundo; plataforma rasa; migração Kirchhoff; deconvolução; correção estática.

Corresponding author: Italo Santos

[1] Universidade Federal do Rio Grande do Norte - UFRN, Post-Graduated Program in Geodynamics and Geophysics (PPGG), Natal, RN, Brazil – E-mail: idantasdsantos@gmail.com
[2] Universidade Federal do Rio Grande do Norte - UFRN, Geology Department (DG), Natal, RN, Brazil – E-mails: moab.gomes@ufrn.br, helenicevital2004@yahoo.com.br
[3] Universidade Federal do Rio Grande do Norte - UFRN, Petroleum Engineering Department (DPET), Natal, RN, Brazil – E-mail: germangca@gmail.com
[4] Serviço Geológico do Brasil - CPRM, Natal, RN, Brazil – E-mail: lopes.vhr@gmail.com

INTRODUCTION

Before being properly processed, both single-channel and multi-channel seismic data do not represent yet the investigated geological substrates (Kluesner et al., 2018). As the registered data comprises reflection events, which represent the limits of the subsurface lithology, and random noises (Russell, 1988), the processing of single-channel seismic data is as indispensable as the processing of multi-channel seismic data. For a more accurate correlation between seismic data and geology, the random noise needs to be suppressed, the signal/noise ratio needs to be increased, and the vertical resolution needs to be improved. Multi-channel seismic data presents the advantage of having the same point on the sampled depth reflector for different offsets (CDP - Common Depth Point technique), considering a medium formed by parallel and horizontal layers (Mayne, 1962). The number of samples from the same point with different offsets facilitates the estimation of a velocity model in each CDP family (Zhou, 2014). Single-channel seismic data does not have this advantage, as it is zero-offset data, which brings limitations regarding the multiplicity of points imaged in the subsurface. As a result, there is not enough information to attain a careful velocity analysis as it is possible on multichannel data.

Another limitation of the single-channel seismic data is related to the noise content in the seismic record. In single-channel marine seismic data, the seismic trace is convolved with coherent noises such as reflections of the bubble effect, ghost reflections, short-period multiples (Duchesne et al., 2007; Kluesner et al., 2018), which leads to the production of a doubtful seismic section, as to the architecture of the subsurface layers (Kluesner et al., 2018). These noises contribute negatively, reducing the vertical resolution.

Faced with so many challenges in high resolution single-channel marine seismic data, the choice of the method by geoscientists is justified because it is easily operated, with low cost, and low processing requirements (Duchesne & Bellefleur, 2007). Besides, a single-channel marine seismic survey produces seismic sections of the most superficial layers with high resolution (Kluesner et al., 2018).

Several studies applied high-resolution single-channel seismic surveys to investigate the sedimentary evolution and the architecture of Quaternary deposits (Cooper et al., 2018; Ronchi et al., 2018; Rangel & Dominguez, 2019). However, the processing flow applied to the data comprises only standard processes, such as spherical divergence and amplitude correction, frequency filters, and average filters (Pepe et al., 2018; Rodrigues et al., 2019; Alves & Mahiques, 2019). Such workflows are ineffective in exploring the characteristics of the sparker source, and removing or suppressing short-path multiples that appear after the primary (Duchesne et al., 2007). The absence of the fundamental stages of the seismic processing means that the effects of the source signature, multiples, and diffractions were not removed or suppressed, which compromises the resolution of the data, besides inducing the interpreter to make ambiguous seismic stratigraphic interpretations (Duchesne et al., 2007).

Some articles were published focusing on single-channel seismic data processing (Alessandrini & Gasperini, 1989; Quinn et al., 1998; Bellefleur et al., 2006; Duchesne & Bellefleur, 2007; Duchesne et al., 2007; Baradello, 2014; Kluesner et al., 2018). However, there is still a need to apply effective processes to suppress the effects of the seismic wavelet, the bubble effect, and the multiples to increase the resolution and the signal/noise ratio and obtain more representative seismic images of the layers in the subsurface comprising their real structure.

The application of deconvolution on single-channel data is another challenge because of the type of deconvolution and its effectiveness, depending on the type of wavelet the seismic source produces. If the seismic source produces a minimum phase wavelet, the spiking deconvolution is the most suitable, as its algorithm uses the assumption that considers the wavelet as a minimum phase (Yilmaz, 2001). If the seismic source produces a mixed-phase wavelet, which is the case of the sparker source, the application of

minimum phase deconvolution is not efficient because the algorithms do not perform well for mixed-phase wavelets (Duchesne et al., 2007).

This work aims to present a processing flow applied to single-channel marine seismic data acquired with sparker acoustic sources exploring primordial stages of the seismic processing such as deconvolution and migration. Deconvolution was applied to reduce the effects of the wavelet and recover the reflectivity function while migration was tested to obtain a seismic image as close as possible to the real geological setting, to reposition the reflectors to their actual subsurface positions and to increase the signal ratio/noise, thus facilitating data interpretation.

STUDY AREA

The southern continental shelf of Bahia state, next to the Jequitinhonha River delta, is within the context of the Jequitinhonha Basin, deposited on the São Francisco Craton (Alkmim et al., 2001; Dominguez et al., 2013), in Central-East Brazil Continental Margin (Fig. 1). This basin is limited to the north by Olivença High and to the south by Royal Charlotte Bank (Rangel et al., 2007).

Bahia continental shelf is shallow with water depths of ~50 m at shelf break and narrow with width up to 32 km. The shelf widens at south near to the Royal Charlotte and Abrolhos banks (Fig. 1) (Dominguez et al., 2012; Dominguez et al., 2013). In the southern of the Jequitinhonha River delta, the continental shelf is widest, with approximately 200 km (Dominguez et al., 1987).

This developed physiography is controlled by the structural heritage of São Francisco Craton and Araçuaí Neoproterozoic Fold Belt (Fig. 1) (Dominguez et al., 2012; Dominguez et al., 2013) associated with the Gondwana breakup (Davison, 1997; Alkmim et al., 2001). Throughout the Quaternary, sea-level fluctuations and the input of river-derived sediments were major influences on the morpho–sedimentary evolution of the Bahia continental shelf (Dominguez et al., 2013).

Dominguez et al. (2013) reported that most of the off coast deposits derived from the erosion of Mesozoic and Precambrian rocks transported by incised valleys to shelf zones. The inner shelf sediments are dominantly terrigenous, varying in grain size from gravel to mud (Dominguez et al., 1987; Dominguez et al., 2012; Dominguez et al., 2013). Along the coastline, there is a narrow strip of sediments composed predominantly of quartz (76-100%) with grain size ranging from gravel to medium sand. Near to the mouth of the Jequitinhonha River, muddy deposits are limited to a narrow and continuous belt bordering the coast, and to the depressions of incised valleys (Dominguez et al., 2013). In contrast, middle and outer shelves are covered by gravelly bioclastic sediments, comprising coralline algae, foraminifera, mollusks, and bryozoans (Dominguez et al., 2012; Dominguez et al., 2013).

METHODOLOGY

A geophysical survey was carried out in the months of February and March/2013 by the Geological Survey of Brazil (CPRM) using the research vessel Marechal Rondon. The seismic source and the streamer were an Applied Acoustics Squid2000 sparker source discharging at power levels ranging from 2100J to 2500J, operating in a frequency range from 100 Hz to 1200 Hz, with a single-channel streamer containing 8 hydrophones with a distance of 50 cm between the elements. The acquisition geometry used the offset of 4.4 meters between source and streamer. A total of 1500 km of high-resolution seismic lines was acquired. The seismic data was converted to the Seg-Y format.

A segment of the seismic line Long06A (Fig. 1) was chosen and submitted to the processing flow proposed in this study (Fig. 2). Among all lines, this seismic section exhibited a better definition of the seafloor; sufficient penetration and resolution; features such as buried valleys showing internal stratigraphic structures that present great diversity of reflector termination patterns and

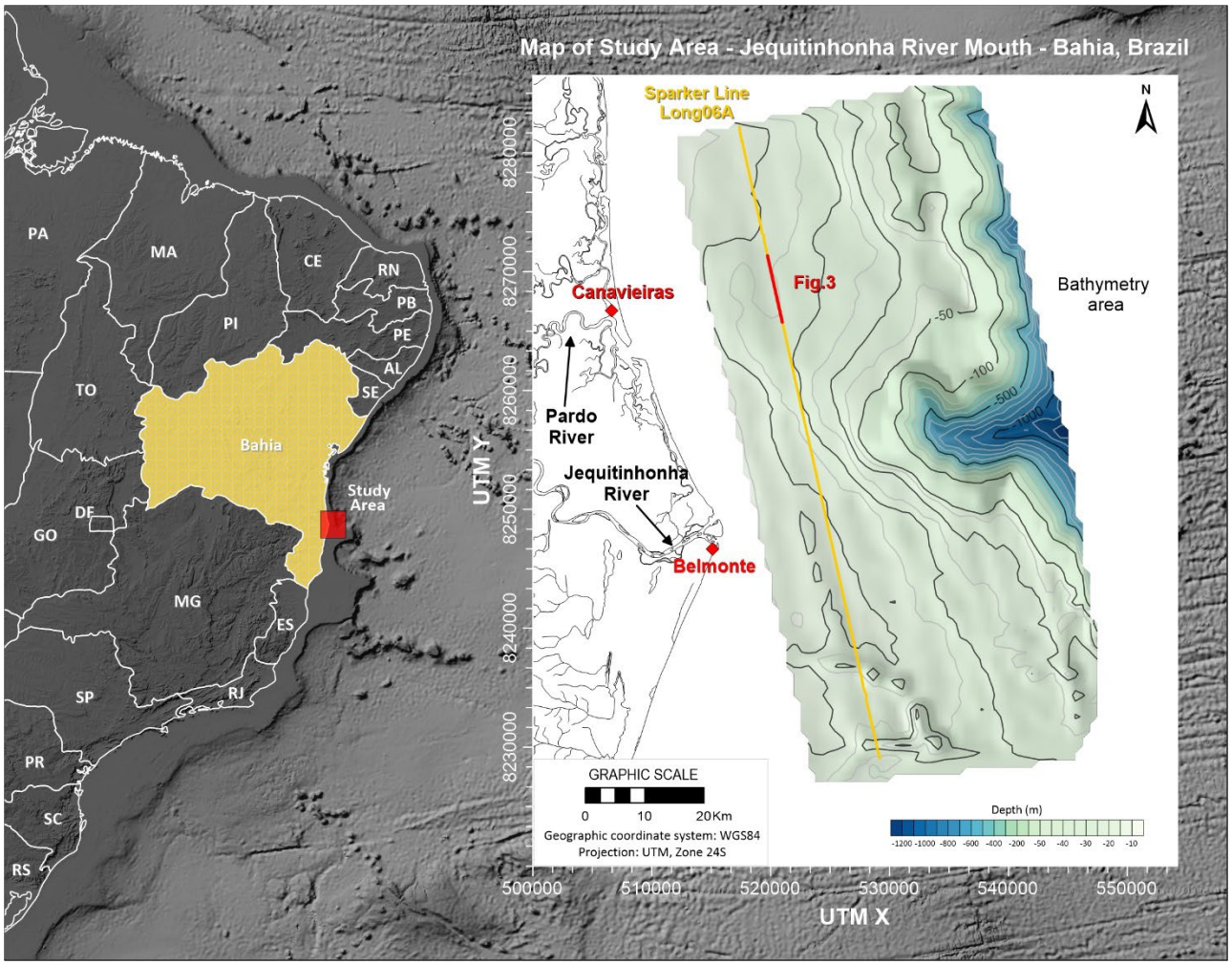

Figure 1 - Study area exhibiting the location of the sparker seismic section. Seafloor topography adapted from Smith & Sandwell (1997) and bathymetry of the study area from Lopes & Frazão (2018).

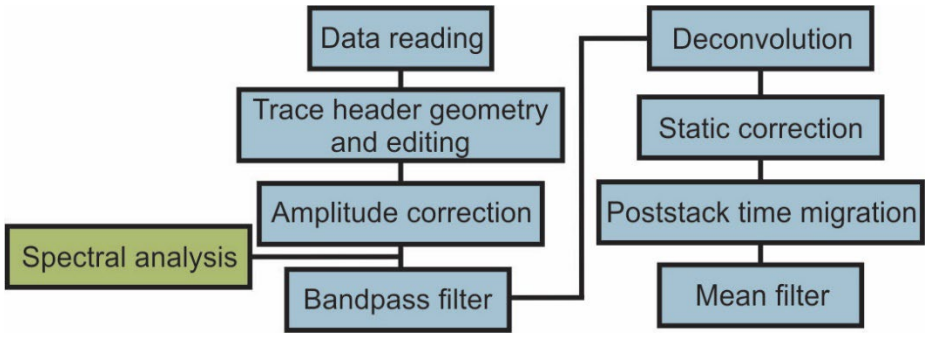

Figure 2 - Proposed seismic processing workflow for single-channel high-resolution seismic data.

inclined surfaces; and the acquisition depths that encompassed the multiple of the seabed with affected and non-affected sedimentary packages. This seismic segment (Profile 01 in Fig. 1) was limited to 5200 traces allowing optimizing the time-consuming of the flow steps before the entire data set be processed.

The processing workflow proposed (Fig. 2) comprises primary (deconvolution and migration) and standard steps (static correction, spherical divergence and amplitude correction, frequency filters, and average filters) based on the routines applied to the conventional hydrocarbon seismic exploration (Yilmaz, 2001). The processing workflow was developed considering the limitations of the sparker single-channel seismic data to image shallow geological structures.

The workflow adaptations include static correction, deconvolution, and migration. When choosing deconvolution algorithms, the particularity of the seismic wavelet must be considered. Besides, a velocity function is essential to apply migration on multichannel data. The velocity function results from the velocity analysis based on the information from CDP gathers. For single-channel data, the velocity analysis was adapted by testing velocity values while applying migration. The velocity value that collapses the hyperbolas is the closest value for the layer. The software used to process the seismic sections was *ReflexWin 7.2.3* (K. J. Sandmeier).

RESULTS AND DISCUSSIONS

The proposed workflow is organized in eight steps and one subdivision. The processing was applied to the strike seismic section of the continental shelf, Profile 01 (Fig. 1).

Data reading

The raw seismic data in the Seg-Y format is converted to the internal format (32-bit floating point) of the ReflexWin software for data visualization through the 2D data analysis module and the definition of the scale patterns. In this step, the data visualization is configured for color palette and scale. The data manipulation at this stage is not permanent. It does not generate processed output data. Thus, it is possible to modify the color palette, trace normalization (or wiggle), scale, gain ratio of amplitudes, and contrast for instantaneous visualization.

Trace header geometry and edition

In single-channel seismic data, the geometry parametrization is considerably less complex, since the survey is single-channel on which the source and receiver are arranged in the same position, resulting in a zero-offset section. Considering the offset between the source and streamer of 4.4 meters of our data, we calculate the time zero t0, the water depth, and the reflection angle. Applying a velocity value of 1500 m/s and the double reflection time of the water/seafloor interface of approximately 0.035 s, we estimate 0.034 s for the zero time t0. The difference between t and t0 is around 0.001 s. Afterward, we calculate the water depth of approximately 27 m and the reflection angle of 4.82°. Since the reflection angle is relatively small, the sparker data may be considered as zero-offset seismic data. Another aspect that simplifies this step is the fact that the geographic coordinates are inserted in the header of each seismic trace as the survey goes on.

Profile 01 (Fig. 3) has 5200 traces distributed along 6,260 meters of the seismic section showing a trace increment of 1 m, time increment of 0,05 ms, and maximum recording time of 400 ms. The seismic section shows good penetration up to 160 ms. It was observed that the signal energy loss becomes greater as the propagation time increases. For this reason, we operate a time cut at 160 ms.

Amplitude correction

The amplitude in raw seismic data is not evenly distributed over the entire length of the seismic trace because the arrivals from deeper reflectors have considerably lower amplitudes, while the arrivals from shallower reflectors have higher amplitudes (Dondurur, 2018). The correction of spherical divergence is the process by which the amplitude of the seismic data starts to show uniform distribution both in the shallow and deep part of the section (Dondurur, 2018).

To correct these effects, it was necessary to apply a gain function available in *ReflexWin* (*div. Compensation*), which compensates for the loss of amplitude by acting trace by trace independently. After the *div. compensation*, we observed an improvement in the energy compensation of the reflectors over the entire time axis and, as a result, the reflectors became clearer (Fig. 4)

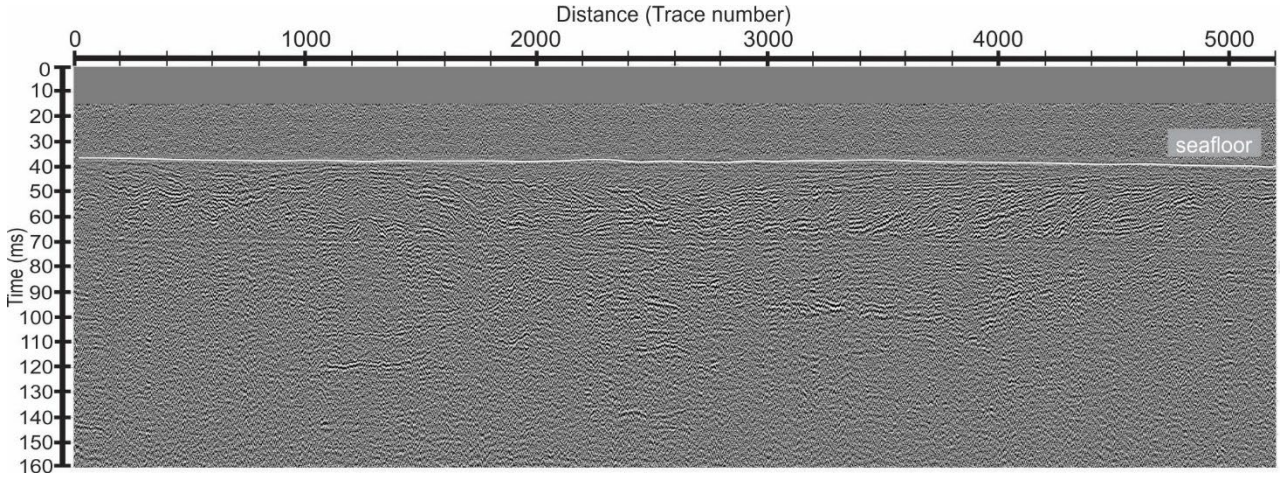

Figure 3 - Raw single-channel sparker data collected on the south Bahia continental shelf.

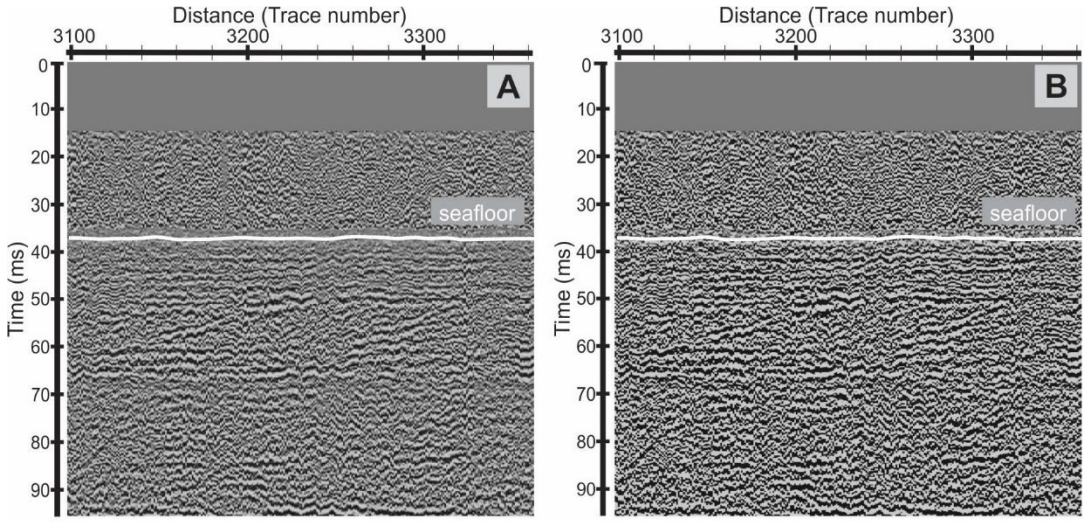

Figure 4 - Amplitude correction by applying the div. compensation tool. Portion of the data (A) before the amplitude correction and (B) after the amplitude correction.

Spectral analysis and Band-pass filter

The spectral analysis of the seismic data shows the frequency spectrum of the data recorded in the time domain (Bath, 1974). Fourier transform is used to transform the waveform of the seismic signal into a function, which contains the amplitude and phase information of the seismic data spectrum.

In the seismic data, the signal and noise amplitudes appear in different frequency components (Yilmaz, 2001; Dondurur, 2018). For this reason, the frequency filtering process may achieve satisfactory results. However, when noise frequencies appear close to the signal frequencies, the signals related to the real reflection events might be subtracted when a frequency filter is applied (Dondurur, 2018).

Incoherent noises from the acquisition environment, instruments, and survey vessel are present in the marine single-channel seismic data (Robinson & Treitel, 2000). A high amplitude swell noise is also present in the marine data, which prevails in the low-frequency range of the data spectrum (Dondurur, 2018). Thus, the frequency range of the swell noise can be removed by applying a band-pass filter.

The data analysis was performed analyzing the amplitude spectrum of the data (Fig. 5). Hence, we estimated the dominant frequency ranges of the data (150Hz - 1500Hz), and estimated the parameter values for the band-pass filter (lower cutoff (150 Hz), lower plateau (400 Hz), upper plateau (1000Hz), upper cutoff (1500 Hz). The swell-noise is a high amplitude noise that normally contains frequencies

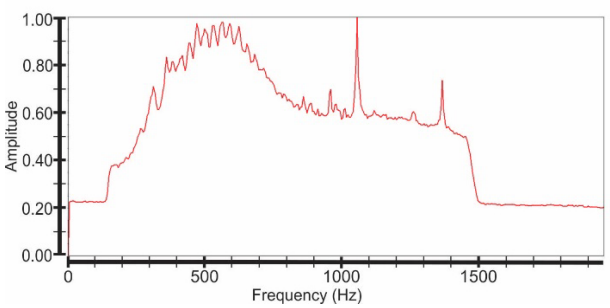

Figure 5 - Amplitude spectrum of the sparker seismic data.

ranging from 2 to 20 Hz (Dondurur, 2018). After identifying the dominant frequency (150Hz - 1500Hz), the band-pass filter with a 150Hz lower cutoff value was applied and suppressed the swell-noise. The band-pass filter result was satisfactory. Low-frequency noises in the spectrum below 150 Hz and above 1500 Hz were removed (Fig. 6). There was an improvement in the signal/noise ratio and a strengthen on the subsurface reflectors (Fig. 6).

Deconvolution

The primary purpose of a seismic reflection survey is to recover the reflectivity function of the investigated area. Deconvolution is the ideal tool for this recovery since by convolving the seismic trace with its inverse filter, we reconstruct the reflectivity function of the geological environment investigated. However, the reality in most surveys is that the wavelet is unknown. Thus, deconvolution becomes a statistical problem, requiring inverse filters capable of applying statistical analysis to seismic traces in the time domain (Robinson & Treitel, 2000). This is the case with the predictive deconvolution: a tool applied to suppress, and even eliminate, multiple events based on the theory that multiple reflection events are periodic and predictable from the arrival times of primary reflections (Dentith & Mudge, 2014).

Regarding the predictive deconvolution, two assumptions should be considered: (1) the reflectivity function is random, meaning that the seismic traces contain the characteristics of the seismic wavelet. As a result, the seismic traces show similarity in their autocorrelations and amplitude spectra, which allows us to replace the autocorrelation of the seismic trace by the autocorrelation of the seismic wavelet (Yilmaz, 2001); (2) the wavelet should be a minimum phase wavelet. In this way, it is possible to estimate an inverse filter based on the autocorrelation function of the seismic trace capable of predicting and suppressing predictable periodic components (Yilmaz, 2001).

The application of deconvolution in single-channel seismic data can be limited depending on the type of wavelet the seismic source produces. When the seismic source produces a minimum phase wavelet, the spiking or predictive deconvolution is indicated. The reason is that these deconvolution algorithms use the assumption of a minimum phase wavelet (Yilmaz, 2001). If the seismic source generates a mixed-phase wavelet, the application of a minimum phase deconvolution is inefficient because these algorithms do not perform well when the wavelet is mixed-phase (Duchesne et al., 2007).

A sparker source produces a mixed-phase wavelet, which fundamentally differs from the chirp and boomer sources. We applied the predictive deconvolution based on the Wiener filter, aiming to remove the multiples. For the predictive deconvolution, the length of the inverse filter operator and the best lag values were set to 60 ms and 3 ms, respectively. The predictive deconvolution was not effective in collapsing the source wavelet for sparker data. This was already expected because it is not the task of the predictive deconvolution to remove the effects of the source wavelet (Duchesne et al., 2007). The predictive deconvolution did not remove the multiple but slightly attenuated it (Fig. 7). Moreover, the deconvolution removed the high-frequency noise (Fig. 8) and increased the frequency

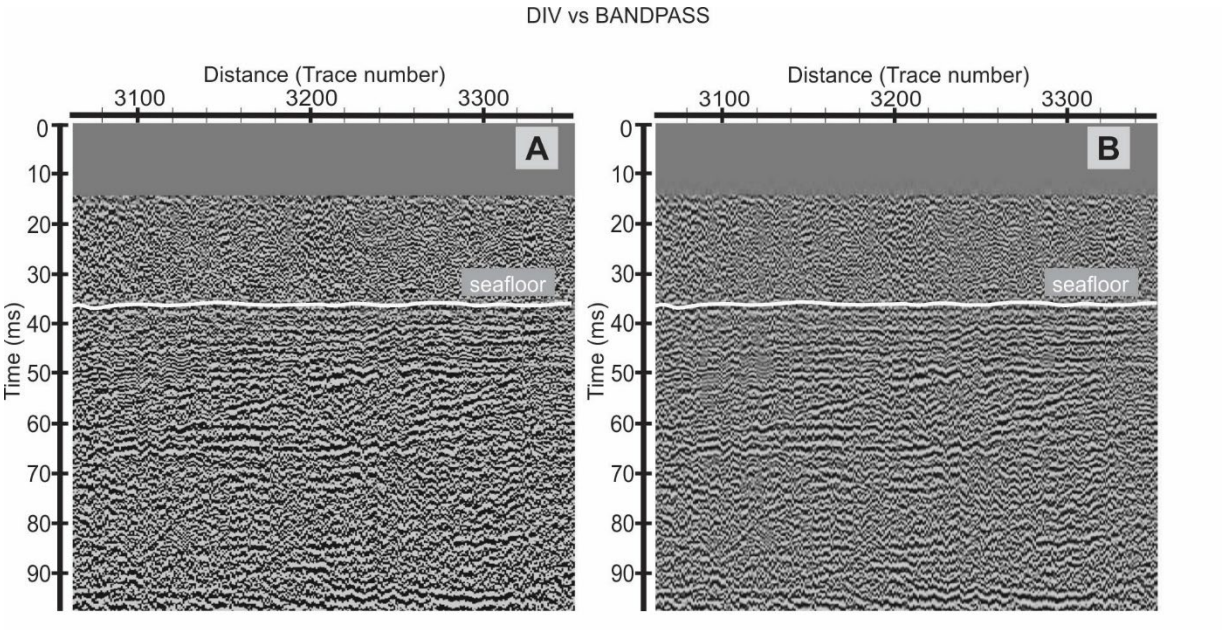

Figure 6 - Application of the band-pass filter. (A) Data before the band-pass and (B) after the band-pass filter application.

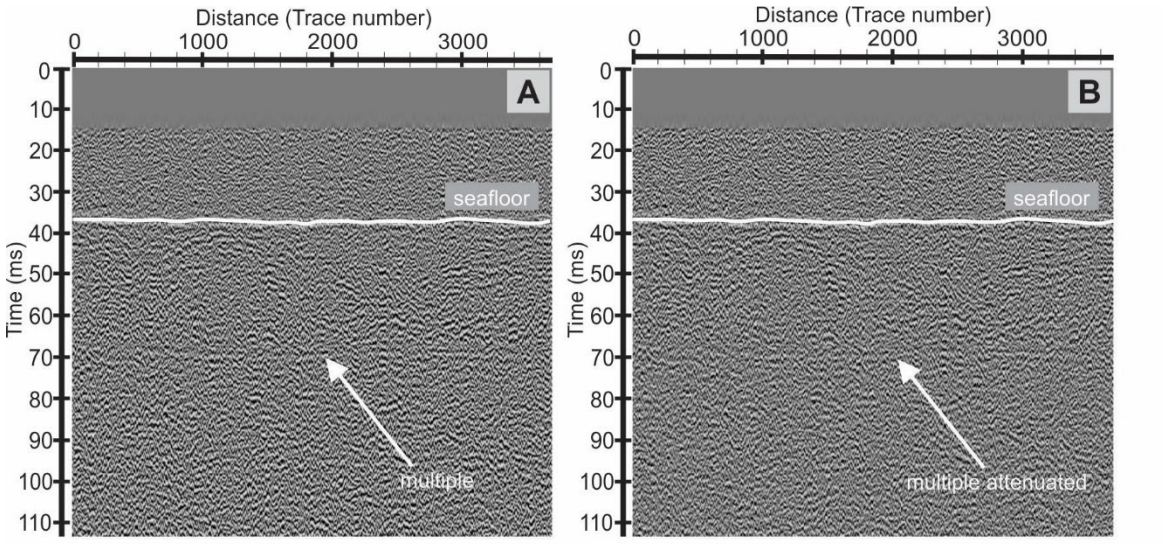

Figure 7 - Comparison between the band-pass filter result (A) and the result of the predictive deconvolution (B) showing the multiple attenuation.

spectrum of the data as indicated by the circles (Fig. 9).

The frequency spectrum analysis of the raw and processed data (Fig. 9) provided a considerable improvement by removing high-frequency noises from the raw data. In the raw data frequency spectrum (Fig. 9A), the high-frequency peak is indicated by the black arrows in addition to a serrated effect present throughout the graph. This effect is a result of the high-frequency noise in the data. In Figure 9B, we noticed that both the high-frequency peak and the notched effect in the frequency graph have been smoothed, which means that deconvolution has attenuated the high-frequency components, although it is not a deconvolution task.

Static correction

In single-channel shallow seismic data, it is common to observe wavy reflectors (Kluesner et al., 2018). This effect is generated due to the action of tides, waves, which cause changes in

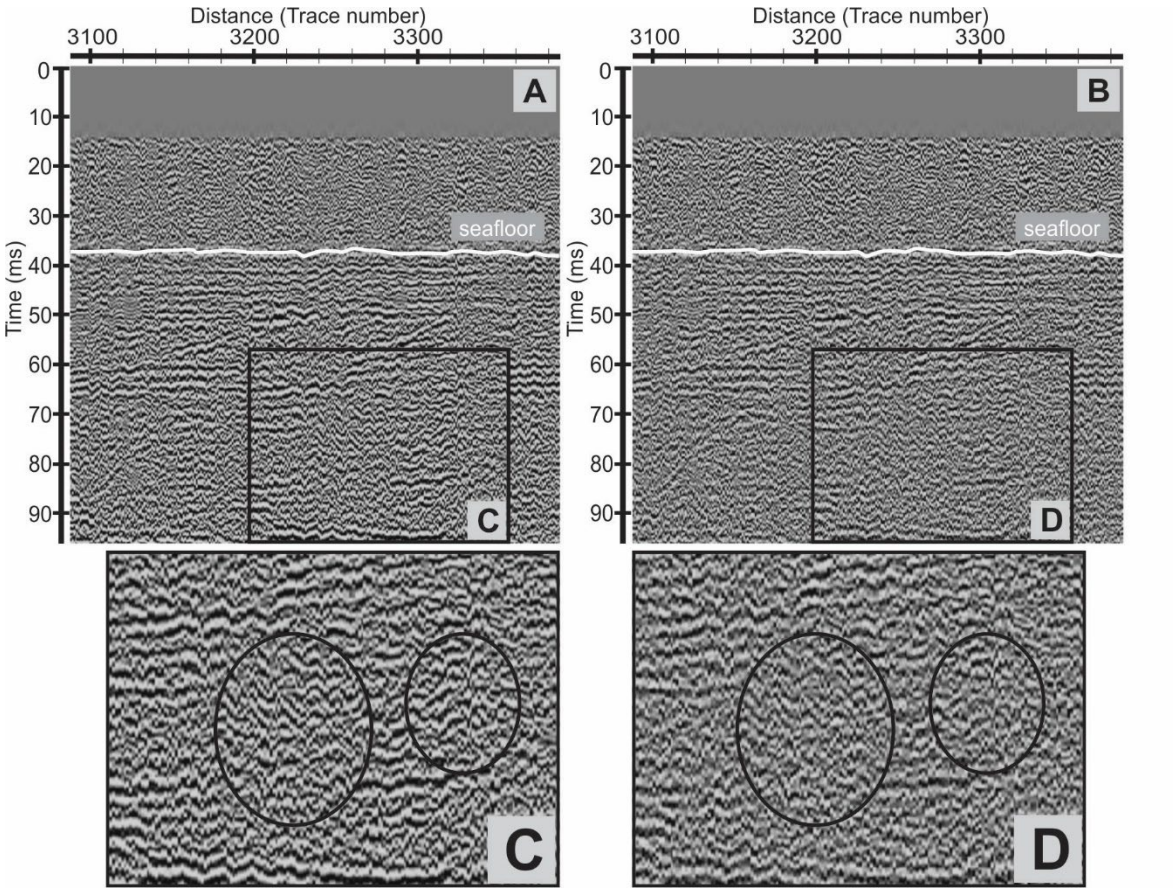

Figure 8 - Comparison between the raw seismic data (A) and the result of the predictive deconvolution (B). In (C) zoom of the raw data showing high-frequency noises and (D) the zoom of the same area after application of the predictive deconvolution.

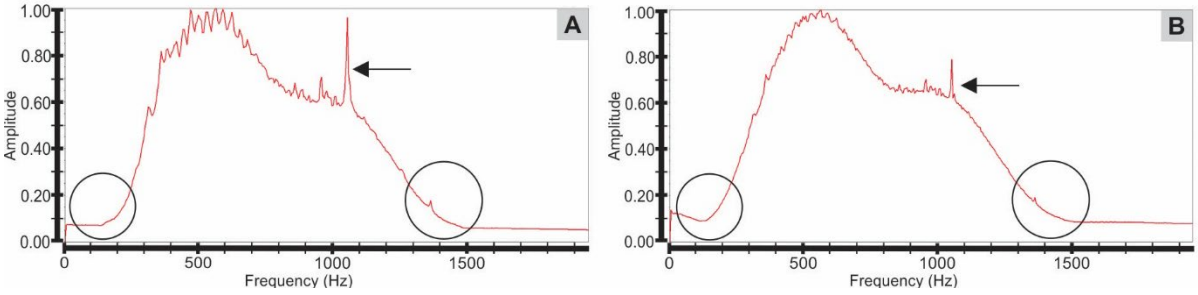

Figure 9 - Amplitude spectrum of the data before the predictive deconvolution (A) and amplitude spectrum of the deconvolved sparker seismic data (B).

the water column height, affecting the elevation of the sea surface (Lacombe et al., 2009; Kim et al., 2017). All of these factors influence the round trip of the seismic pulse producing a lateral discontinuity in the seismic section, which compromises the visualization of the investigated structures in the subsurface. To correct these errors, it is necessary to apply the static correction.

In this work, the static correction was applied using resources from the *ReflexWin* and *OasisMontaj* softwares. This process comprises three stages: (1) picking the seabed surface reflector; (2) removing water column and displacing traces to zero time; (3) smoothing the seabed surface in the *OasisMontaj* software and incorporating the smoothed surface into the seismic section in the *ReflexWin*. The static correction produced satisfactory results smoothing the seabed reflector, reducing the undulated and chaotic patterns, and improving the lateral continuity of the reflectors (Fig. 10). Furthermore, the static correction provided better conditions for the application of the post-stack time migration, which resulted in coherent seabed surface and subsurface reflectors.

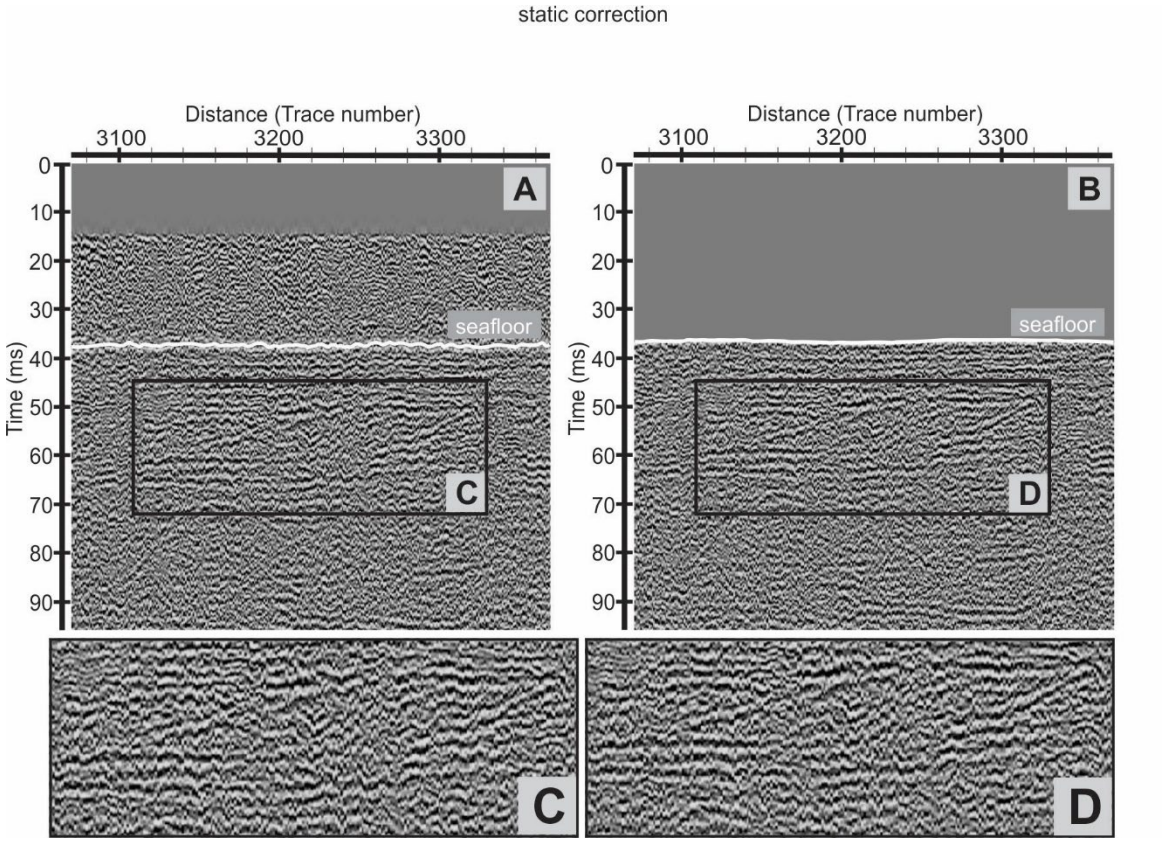

Figure 10 - A portion of the sparker section. (A) Data before static correction. (B) Data after static correction. (C) Zoom of the data before static correction and (D) zoom of the data after static correction.

Migration

The purpose of migration is to generate a more accurate seismic image of the subsurface by moving reflectors to more realistic positions in the subsurface and collapsing diffractions (Yilmaz, 2001; Dentith & Mudge, 2014). In this research, the sparker single-channel data is zero-offset, similar to a stacked zero-offset section of the conventional seismic. Among the available migration strategies, the Kirchhoff method was applied because it allows migrating common-offset (CO) sections, being zero-offset (ZO), a particular case of the CO geometry (Bancroft, 2007). The use of the post-stack time migration requires a velocity function. We tested velocity values from 1450 m/s to 2200 m/s based on standard velocity values for water-saturated sediments (Schumann et al., 2014). However, the best result to collapse the diffraction hyperboles occurred with the value of 1550 m / s. We applied a velocity value of 1550 m/s for the entire sediment column. Even using a simple 1D stratified velocity model, Kirchhoff post-stack time migration was efficient by enhancing seafloor and subsurface reflectors. Figures 11, 12, and 13 show the data improvements by noise reduction and the repositioning of dipping reflectors. Furthermore, the migrated data provides a section revealing numerous clear, coherent, and distinguishable reflectors. Before the Kirchhoff migration application, the same reflectors were distorted (Figs. 11A and 12A). The application of Kirchhoff migration collapsed the diffraction hyperbolas along the seismic sparker section (Figs. 11 and 12) and proved to be essential to obtain an accurate image of the continental shelf subsurface. Moreover, it resulted in a coherent image, which revealed stratigraphic details of the south Bahia continental shelf (Fig. 15).

Trace average filter (Mean filter)

The mean filter operates on each trace independently by performing an average based on a selectable number of time samples. To calculate an average of the amplitudes of a trace, it is necessary to inform the filter parameter 'mean range'. The mean filter was used for constructive averaging the recorded signal. The application of

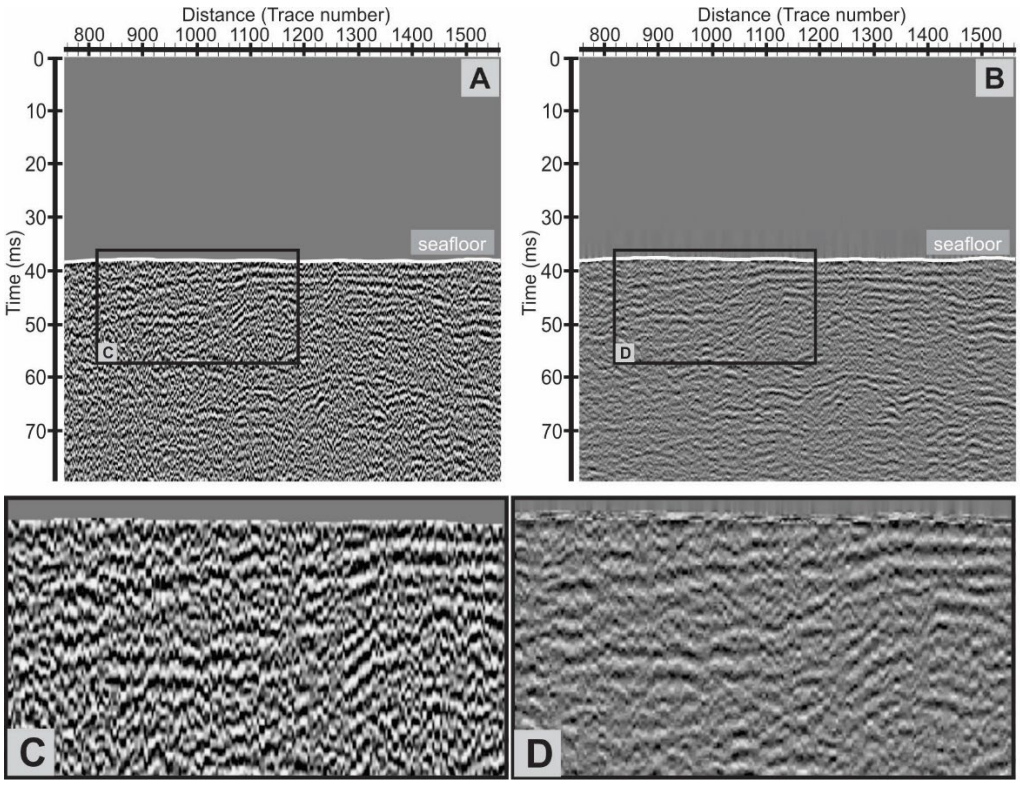

Figure 11 - Comparison between non-migrated sparker seismic data (A) and the result of Kirchhoff migration (B). In (B) we highlight in the rectangles the collapse of diffraction hyperbolas, the increase in lateral continuity of the reflectors, and the repositioning of the reflectors. In (C) zoom of the data before migration and (D) zoom of the data after migration.

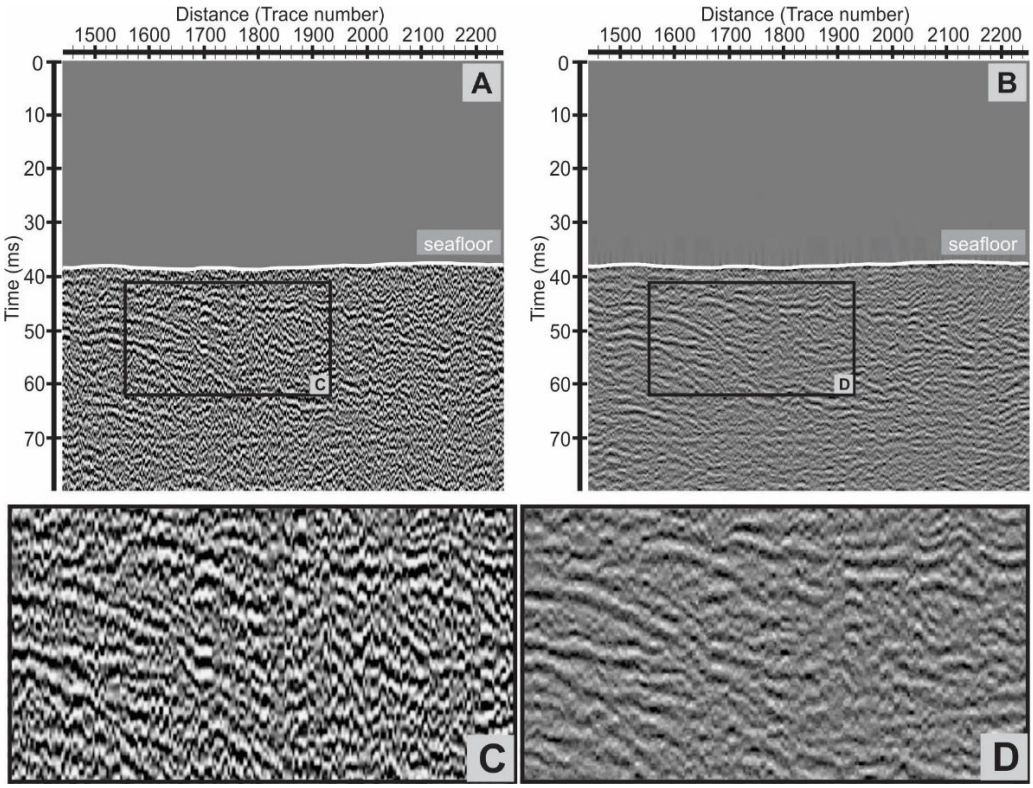

Figure 12 - Comparison of another portion of the sparker seismic data between the non-migrated section (A) and the result of the Kirchhoff migration (B). In (B) the diffraction hyperbolas were collapsed and dipping reflectors were repositioned. In (C) zoom of the data before migration and (D) zoom of the data after migration.

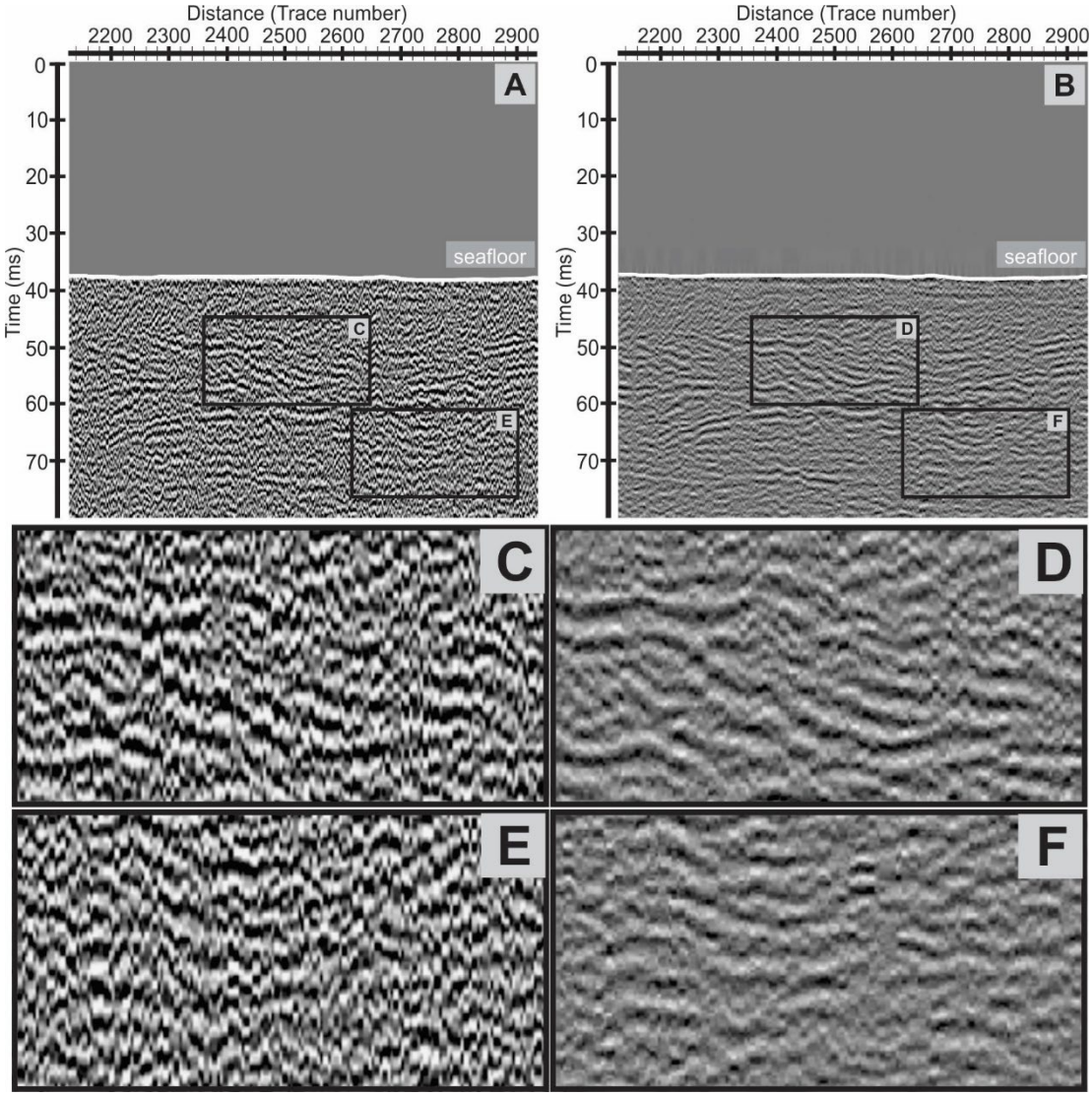

Figure 13 - (A) non-migrated section and (B) Kirchhoff migrated section. In (A) the rectangles highlight the distorted reflectors and the chaotic pattern. In (B) we notice an evident improvement of the distorted reflectors with the lateral continuity enhancement, repositioning of reflectors, and reduction of noise. In (C) and (E) zoom of the data before migration and (D) and (F) zoom of the data after migration.

the mean filter improved the lateral continuity due to the reduction of the noise between the traces and, consequently, enhanced the coherency in the data, reduced the high-frequency noises and the undulated effect on the reflectors (Fig. 14). The application of a three-trace window average trace filter resulted in the constructive average of the seismic data.

The processing flow capacities

Figure 15 shows the complete processed seismic section resulted from the segment seismic line in Figure 2. The resulting section (Fig. 15) exhibits a seismic image with high vertical resolution revealing the architecture of the Quaternary sedimentary deposits on the south Bahia continental shelf. When processing single-channel sparker seismic data, Bellefleur et al. (2006) applied trace-by-trace deconvolution designed for vertical seismic profiles (VSP deconvolution) to attenuate the bubble pulse produced by the sparker source signature. For this purpose, a filter was designed to convert the sparker mixed-phase wavelet into a minimum phase wavelet. As a result, the processing strategy produced the output data by collapsing the sparker signature. However, the multiples were not completely attenuated.

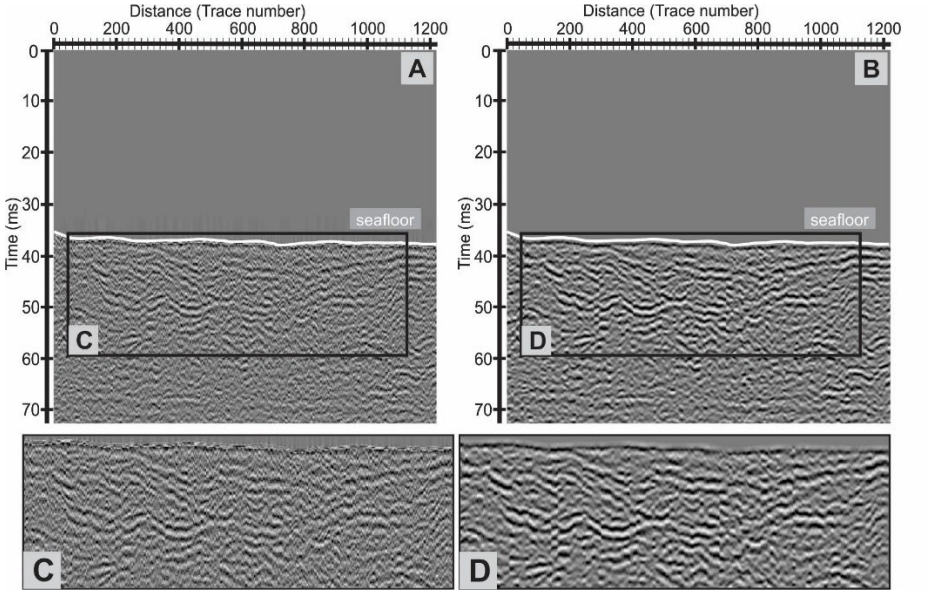

Figure 14 - Comparison between the result of Kirchhoff migration application (A) and the result of the mean filter application (B). In (C) zoom of the data before mean filter application and (D) zoom of the data after mean filter application.

Duchesne and Bellefleur (2007) proposed some strategies for the attenuation of source signature in sparker data, among which the matched-filter and the VSP deconvolution produced the most satisfactory results. The application of the matched-filter requires that seafloor reflections be converted to a minimum phase. After that, the idea is to use the seafloor reflections matched-filtered converted to a spike to design a trace-by-trace operator. The application of the matched-filter removed the multiples associated with seafloor and bedrock primaries and increased the vertical resolution.

Baradello (2014) proposed a deconvolution strategy for uncorrelated Chirp data. The strategy aims to design an inverse filter capable of converting the Chirp sweep into an equivalent minimum-phase wavelet. Obtaining an equivalent minimum-phase wavelet occurs from uncorrelated Chirp data. The predictive deconvolution was applied to both the envelope chirp data and the minimum-phase chirp data. The results of both applications showed that for the envelope chirp data, the predictive deconvolution attenuated multiples, but it did not increase the vertical resolution, while for the minimum-phase chirp data, the predictive deconvolution increased the vertical resolution and reduced the ringing noise on reflectors. On the other hand, results presented by Gomes et al. (2011) showed that the application of predictive deconvolution on the envelope chirp data attenuated the seabed multiples without compromising the amplitude of deeper reflectors.

Gomes et al. (2011) and Teixeira & Ayres Neto (2017) proposed processing workflows applied to chirp envelope data. This seismic source has wavelet particularities, which differ from those generated by boomer and sparker sources. For instance, the choice of the deconvolution algorithm depends essentially on the source signature. Chirp systems produce a frequency modulated sweep (Baradello, 2014). The full knowledge of the chirp sweep is an advantage in choosing the appropriate deconvolution algorithm to process the data. The deterministic algorithms applied to Vibroseis data compose the same strategy to approach uncorrelated chirp data (Baradello, 2014). Once the chirp data is enveloped, the phase information is lost and the deconvolution processing becomes limited to the predictive deconvolution applied to suppress seafloor multiples. Besides, the unrecoverable phase information violates the assumption of wave equation compliance (Baradello et al., 2021). Thus, migration algorithms, which are based on the full-wave equation, will not be effective.

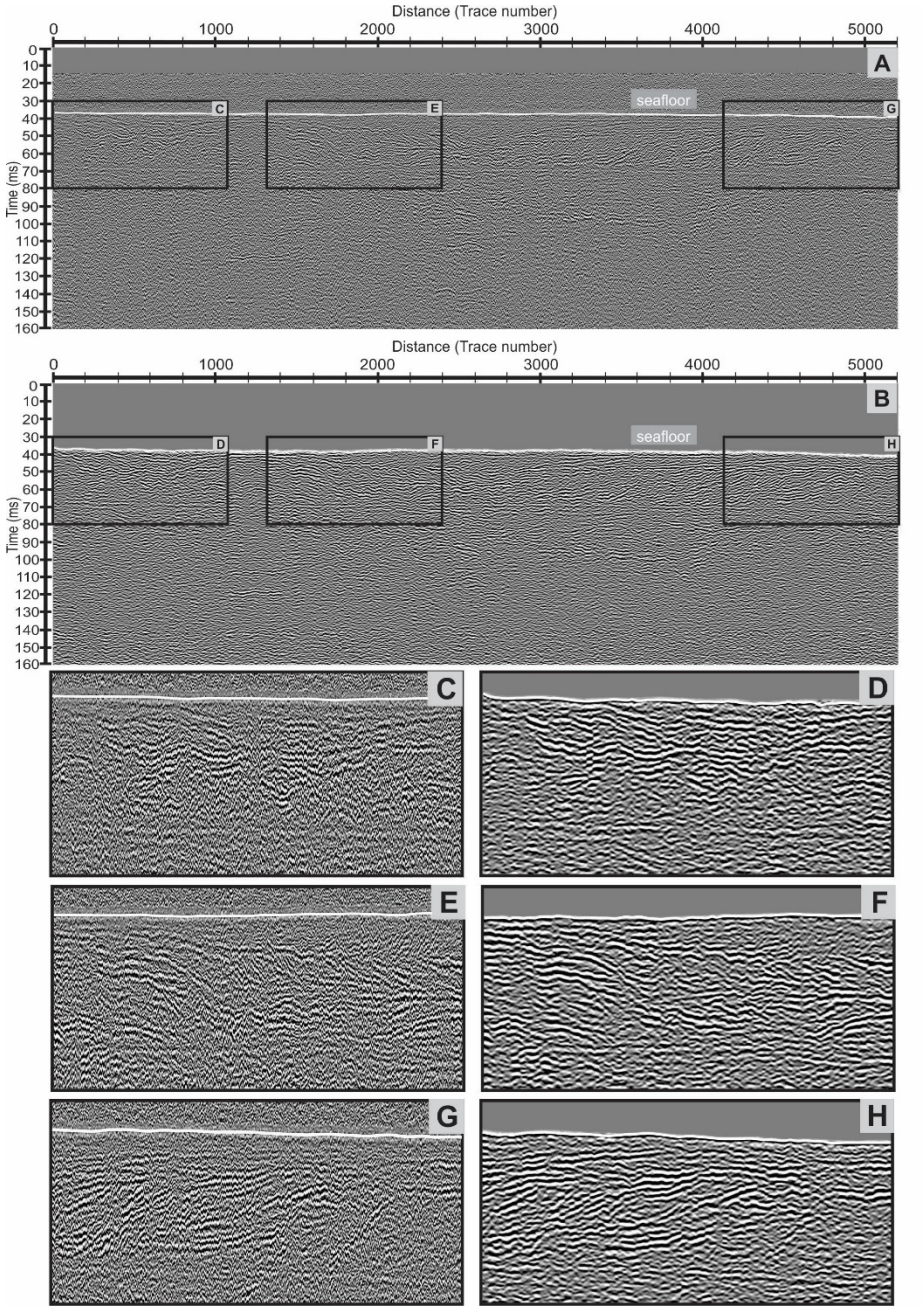

Figure 15 - Comparison between the raw seismic section (A) and the migrated single-channel sparker seismic image (B) exhibiting high vertical resolution. In (C), (E), and (G) zoom of the raw data and (D), (F), and (H) zoom of the processed data.

In contrast, the sparker systems produce a mixed-phase wavelet, which implies that deconvolution algorithms based on the Wiener filter are not efficient to collapse wavelet effects, because to suppress sparker mixed-phase wavelet requires specific strategies, such as mixed-phase deconvolution. However, the predictive deconvolution still may attenuate the multiples (Kluesner et al., 2018). Furthermore, the full-waveform from sparker seismic data allows the employment of migration algorithms. The present processing workflow includes static correction, absent in the previous processing attempts (Gomes et al., 2011; Teixeira & Ayres Neto, 2017), and specific steps to the sparker sources such as deconvolution and migration, which provided significant improvements in the quality of the seismic image.

This study had no access to algorithms capable of calculating an operator to convert a mixed-phase wavelet into a minimum-phase one or to mixed-phase deconvolution algorithms.

Attempting to apply predictive deconvolution failed in collapsing the source wavelet. This result confirms the approach of Duchesne et al. (2007) (which suggests using minimum-phase conversion to compress the sparker source wavelet) and the proposal of Kluesner et al. (2018) (the use of mixed-phase deconvolution algorithms). Although failing in collapsing the source wavelet and removing the multiples, the predictive deconvolution slightly attenuated the multiples.

A serious issue in sparker seismic data is random noises caused by waves and currents. The removal of random noises is crucial for the improvement of the signal/noise ratio because it compromises vertical resolution and, consequently, the signal/noise ratio. The results confirm that the combination of the band-pass filter and predictive deconvolution followed by the static correction attenuated the random noises, as well as improved the lateral continuity of reflectors.

The static correction smoothed the seabed reflector and the undulated/chaotic pattern on the subsurface reflectors. Despite being considered a standard step in seismic processing, the static correction showed significant results correcting the effects generated by static variations as expected. Besides, the static correction preconditioned the data to apply post-stack time migration. For this reason, the static correction must be inserted into the high-resolution marine seismic data processing flow.

Figures 11, 12 and 13 demonstrate that migration constitutes a fundamental processing step technique that should be adopted in the application of single-channel high-resolution seismic data processing. Clearly, the application of the post-stack time migration enhanced the lateral continuity and coherence of the seabed reflector and subsurface ones. Figures 11, 12, and 13 confirm the repositioning of dipping reflectors close to real position, the collapsing of diffraction events, and the reduction of noise, and the correction of distorted reflectors, which resulted in a section with higher resolution.

The processing techniques discussed in this study can be applied on a chirp envelope data, although they will not produce seismic sections with vertical resolution such as those produced by the approach of Baradello (2014), which is applied to uncorrelated chirp data. The application of the processing flow proposed by this study in boomer data will certainly collapse the boomer signature (since boomer produces a minimum-phase wavelet) and will result in seismic sections with a higher signal/noise ratio and vertical resolution than the raw boomer data.

CONCLUSION

This study presented a proposal of a processing sequence applied to single-channel marine seismic data from sparker acoustic source emphasizing the importance of fundamental stages of seismic processing such as deconvolution and migration. The results highlight the relevance of applying seismic processing routines to produce a more accurate sparker single-channel seismic image for interpretation.

The application of conventional deconvolution techniques based on the Wiener filter on sparker data has shown no effectiveness in collapsing the wavelet recorded in the seismic data. However, the predictive deconvolution slightly attenuated the seabed multiple, removed random and high-frequency noises, and broadened the frequency spectrum of the data.

The static correction proved its effectiveness by correcting the undulated effect on the reflectors caused by static variations. The static correction smoothed the seabed and subsurface reflectors, which preconditioned the sparker data to post-stack migration. The static correction followed by the post-stack migration and the trace average filter improved the trace-to-trace consistency and lateral continuity of the reflectors, besides suppressing random noises. For this reason, the static correction must be considered when processing high-resolution marine seismic data.

Kirchhoff migration collapsed the diffraction hyperbolas along the seismic section. As a result, the sparker data was improved by reducing random noises and repositioning the dip reflectors close to their real position. Moreover, the results presented in this paper corroborate to the efficiency of the proposed processing workflow by providing a high signal/noise ratio image that reveals details of the seismic stratigraphy of the Bahia continental shelf. The trace average filter (mean filter) showed effectiveness in reducing the random noise between the traces and enhancing the lateral continuity and the coherency in the data by using a three-trace window.

The Matched-filter and Mixed-phase deconvolution are appropriate effective techniques to be applied to the sparker data. The Mixed-phase algorithm has been shown to be effective in collapsing the signature of the sparker source and removing the effects caused by a mixed-phase wavelet. Despite proving satisfactory results with the mixed-phase deconvolution, these algorithms are exclusively available in expensive commercial processing packages.

AKCNOWLEDGEMENTS

The authors are extremely thankful for CAPES, for providing the scholarship for the first author; Lab. GGEMMA; PPGG/UFRN, for the academic and scientific infrastructure; and CPRM (Geological Survey of Brazil), for providing the seismic data. The second author MPG thanks CNPq for his research grant (PQ 302483/2019-5).

REFERENCES

ALESSANDRINI B & GASPERINI M. 1989. The deconvolution of marine seismic source: an iterative approach. Geophysics, 54:780-784.

ALKMIM FF, MARSHAK S & FONSECA MA. 2001. Assembling West Gondwana in the Neoproterozoic: clues from the São Francisco craton region, Brazil. Geology, 29: 319-322.

ALVES DPV & MAHIQUES MM. 2019. Deposition and sea-level evolution models for Upper Pleistocene/ Holocene in the São Sebastião Channel (SE Brazilian coast) inferred from 5th order seismic stratigraphy. Journal of South American Earth Sciences, 93:382-393.

BANCROFT, J. C. 2007. A practical understanding of Pre- and Poststack migrations: volume 1 (Postsatck). Tulsa, USA: Society of Exploration Geophysicists. 518 pp.

BARADELLO L. 2014. An improved processing sequence for uncorrelated Chirp sonar data. Marine Geophysical Research, 35:337-344.

BARADELLO L, BATTAGLIA F & VESNAVER A. 2021. Fast method to transform chirp envelope data into pseudo-seismic data. Marine Geophysical Research, 42:14.

BATH M. 1974. Spectral analysis in Geophysics. Amsterdam, Netherlands: Elsevier Scientific Publishing Co. 1-15 pp.

BELLEFLEUR G, DUCHESNE MJ, HUNTER J, LONG BF & LAVOIE D. 2006. Comparison of single- and multichannel high-resolution seismic data for shallow stratigraphy mapping in St. Lawrence River estuary, Quebec. Geological Survey of Canada, Natural Resources Canada, Current Research 2006-D2. p. 1-10.

COOPER JAG, MEIRELES RP, GREEN AN, KLEIN AHF & TOLDO EE. 2018. Late Quaternary stratigraphic evolution of the inner continental shelf in response to sea-level change, Santa Catarina, Brazil. Marine Geology, 397:1-14.

DAVISON IAN. 1997. Wide and narrow margins of the Brazilian South Atlantic. Journal of Geological Society, 154: 471-476.

DENTITH M & MUDGE ST. 2014. Geophysics for the mineral exploration geoscientist. New York: Cambridge University Press. 372 pp.

DOMINGUEZ JML, MARTIN L & BITTENCOUT ACSP. 1987. Sea-level history and the Quaternary evolution of river mouth-associated beach-ridge plains along the east-southeast Brazilian coast: A summary. In: NUMMEDAL D, PILKEY OH & HOWARD JD. Sea-Level Fluctuation and Coastal Evolution. SEPM Society for Sedimentary Geology, 41: 115-127.

DOMINGUEZ JML, NUNES AS, REBOUÇAS RC, SILVA RP & FREIRE AFM. 2012. Plataforma

Continental do Estado da Bahia. In: BARBOSA JSF, MASCARENHAS JF, CORRÊA-GOMES LC, & DOMINGUEZ JML & SOUZA JS. (Eds.). Geologia da Bahia – Pesquisa e Atualização. Salvador, BA, Brazil: CPBM; UFBA. V. 2. Chapter XVIII. p. 427-496.

DOMINGUEZ JML, SILVA RP, NUNES AS & FREIRE AFM. 2013. The narrow, shallow, low-accommodation shelf of central Brazil: sedimentology, evolution, and human uses. Geomorphology, 203: 46-59.

DONDURUR D. 2018. Acquisition and processing of marine seismic data, 1st ed. Oxford: Elsevier. 253-276 pp.

DUCHESNE MJ & BELLEFLEUR G. 2007. Processing of single-channel, high-resolution seismic data collected in the St. Lawrence estuary, Quebec. Geological Survey of Canada, Current Research 2007-D1, p. 11.

DUCHESNE MJ, BELLEFLEUR G, GALBRAITH M, KOLESAR R & KUZMISKI R. 2007. Strategies for waveform processing in sparker data. Marine Geophysical Research, 28:153-164.

GOMES MP, VITAL H & MACEDO JWP. 2011. Fluxo de processamento aplicado a dados de sísmica de alta resolução em ambiente de Plataforma Continental. Exemplo: Macau-RN. Revista Brasileira de Geofísica, 29(1): 173-186.

KIM H, LEE GH, YI BY, TOON Y, KIM K, KIM H & LEE SH. 2017. A simple method of correction for profile-length water-column height variations in high-resolution, shallow-water seismic data. Ocean Science Journal, 52:.283-292.

KLUESNER J, BROTHERS D, HART P, MILLER N & HATCHER G. 2018. Practical approaches to maximizing the resolution of sparker seismic reflection data. Marine Geophysical Research, 40: 279-301.

LACOMBE C, BUTT S, MACKENZIE G, SCHONS M & BORNARD R. 2009. Correcting for water-column variations. The Leading Edge, 28:198-201.

LOPES VHR & FRAZÃO EP. 2018. Mapa batimétrico da Bacia de Jequitinhonha, Sul da Bahia. Recife: CPRM, S a.24-Y -A-V.

MAYNE, WH. 1962. Common reflection point horizontal data stacking techniques. Geophysics, 18(6): 927-938.

QUINN R, BULL JM & DIX JK. 1998. Optimal processing of marine high-resolution seismic reflection (Chirp) data. Marine Geophysical Research, 20:13-20.

RANGEL AGAN & DOMINGUEZ, JML. 2019. Antecedent topography controls preservation of latest Pleistocene-Holocene transgression record and clinoform development: the case of the São Francisco delta (eastern Brazil). Geo Marine Letters,1-13.

RANGEL HD, OLIVEIRA JLF & CAIXETA JM. 2007. Bacia de Jequitinhonha. Boletim de Geociências da Petrobras, 15: 475-483.

ROBINSON EA & TREITEL S. 2000. Geophysical signal analysis, Tulsa, USA: Society of Exploration Geophysicists. 481 pp.

RODRIGUES VS, ALVES DPV, JOVANE L & SOUZA LAP. 2019. Seismic Stratigraphy of Trapandé Bay (southern Brazil) to study sea-level changes and deposition evolution in the Upper Quaternary. Brazilian Journal of Geophysics, 37(4): 357-368.

RONCHI L, FONTANA A, CORREGGIARU A & ASIOLI A. 2018. Late Quaternary incised and infilled landforms in the shelf of the northern Adriatic Sea (Italy), Marine Geology, 405:47-67.

RUSSELL BH. 1988. Introduction to seismic inversion methods. Tulsa, USA: Society of Exploration Geophysicists. 178 pp.

SCHUMANN K, STIPP M, BEHRMANN JH, KLAESCHEN D & SCHULTE-KORTNACK D. 2014. *P* and *S* wave velocity measurements of water-rich sediments from the Nankai Trough, Japan. J. Geophys. Res. Solid Earth, 119: 787-805.

SMITH WHF & SANDWELL DT. 1997. Global seafloor topography from satellite altimetry and ship depth soundings. Science, 277: 1957-1962.

TEIXEIRA BT & AYRES NETO A. 2017. Implementation of processing techniques in single-channel high-resolution seismic data. In: Rio Acoustics IEEE/OES Acoustics in underwater Geosciences Symposium, 2017. Rio de Janeiro, RJ, Brazil.

YILMAZ O. 2001. Seismic data analysis: processing, inversion and interpretation of seismic data, 2nd ed, Tulsa, USA: Society of Exploration Geophysicists, 1. 159-190 pp.

ZHOU HW. 2014. Practical seismic data analysis, New York: Cambridge University Press. 42 pp.

I.S.: Writing – original draft; Conceptualization; Methodology; Validation; Investigation; **M.G.:** Writing – Review & Editing; Supervision. Visualization; Conceptualization; Methodology; Validation; Investigation; **G. G.:** Writing – Review & Editing, Conceptualization, Methodology; Validation; **H.V.:** Resources; Investigation; **V.L.:** Conceptualization; Methodology, Investigation.

Received on April 16, 2021 / Accepted on August 25, 2021